Journal of Materials Chemistry A

Accepted Manuscript

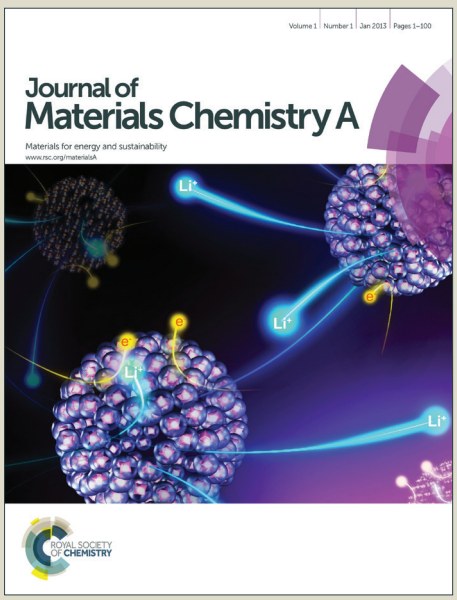

ROYAL SOCIETY OF CHEMISTRY

www.rsc.org/materialsA

Journal of Materials Chemistry A

RSCPublishing

ARTICLE

$KFeSbTe_3$: a quaternary chalcogenide aerogel for preferential adsorption of polarizable hydrocarbons and gases

Cite this: DOI: 10.1039/x0xx00000x

Ejaz Ahmed and Alexander Rothenberger*

Received 00th January 2012,
Accepted 00th January 2012

DOI: 10.1039/x0xx00000x

www.rsc.org/

The first telluride-based quaternary aerogel $KFeSbTe_3$ is synthesized by a sol-gel metathesis reaction between $Fe(OAc)_2$ and K_3SbTe_3 in dimethyl formamide. The aerogel has an exceptionally large surface area 652 m^2/g which is amongst the highest reported for chalcogenide-based aerogels. This predominantly mesoporous material shows preferential adsorption for toluene vapors over cyclohexane or cyclopentane and CO_2 over CH_4 or H_2. The remarkably high adsorption capacity for toluene (9.31 mmol/g) and high selectivity for gases (CO_2/H_2: 121 and CO_2/CH_4: 75) suggest a potential use of such materials in adsorption-based separation processes for the effective purification of hydrocarbons and gases.

Introduction

Hydrocarbons play an essential role in chemical and petrochemical industries. Therefore, improvement in the purification or separation of these solvents for industrial purpose gave rise to modern separation techniques.[1,2] Several procedures have been developed for their effective separation or purification, for example solvent extraction, distillation and adsorption processes.[1,2] Currently, distillation is being practiced for more than 90 % of all separation processes at the industrial level.[3] However, the risk of product decomposition, the reactivity of certain substances as well as the high energy costs associated with distillation highlight the need for alternative separation processes.[1-4] Adsorption is a reliable alternative method which provides an easy and economical way for separation of a wide range of substances in chemical, petrochemical and pharmaceutical industries.[2] Depending upon the interaction between the adsorbent and the constituents of a mixture, an adsorbent is capable to separate a mixture into pure compounds.[5] The characteristics of the adsorbent determine the separation efficiency. Porous materials such as zeolites, silica gel and activated carbon,[6] molecular sieves,[7] polymeric resins,[8] composite materials,[9] and metal-organic frameworks[3,10] have already been investigated for adsorptive separations.

Recently, we have started studies on the adsorption of volatile hydrocarbons using aerogels made from metal chalcogenides.[11] Such chalcogels are predominantly mesoporous materials constructed from inorganic building blocks to yield a three-dimensional network comprising high surface area, large pore size distribution, surface polarizability, and chemical selectivity.[11-21] These characteristic features make chalcogels promising candidates for catalysis,[15] ion-exchange,[18] heavy metal aqueous waste remediation,[21] and selective gas as well as hydrocarbon adsorption.[11,16,19,20] Chalcogenide-based aerogels are easily accessible using the sol-gel method. It has been recognized that the presence of electron-rich chalcogenide ions $[Q_x]^{2-}$ (Q = S, Se, Te; x = 1-5) on the internal surface of the material can increase the surface polarizability. As a result, interaction of the polarizable adsorptives with the surface of the chalcogenide-based aerogels is stronger than interactions with conventional aerogels like organic polymers, carbons, and metal oxides.[15,19]

The key aspects of the sol–gel process have been investigated by Kanatzidis and co-workers.[14-16] They optimized reaction conditions for the gelation from solution, which is a prerequisite for aerogel formation. In case of chalcogenides, gelation is the key step and very often, a high reaction rate leads to rapid precipitation. Different metal acetates and acetylacetonates have been successfully employed in reactions with chalcogenido anions avoiding rapid metal chalcogenide precipitation and allowing gel formation over the course of several days.[11,16,18a,19] A series of chalcogenide aerogels has been described using inorganic building blocks of the main group elements such as tetrahedral clusters ($[MQ_4]^{4-}$ and $[M_2Q_6]^{4-}$, M = Sn, Ge; Q = S, Se)[14,16] adamantane clusters ($[M_4Q_{10}]^{4-}$, M = Sn, Ge; Q = S, Se),[14,16] ditopic linear polychalcogenido anions (S_x^{2-}; x = 3–6),[11a, 18] and trigonal pyramidal anions ($[ES_3]^{3-}$, E = As, Sb).[11b] Furthermore, binary metal sulfides like tetrahedral anions ($[MS_4]^{2-}$, M = Mo, W) or the triangular molybdenum sulfide cluster $[Mo_3S_{13}]^{2-}$ have already been applied as starting materials.[15,19] The family of chalcogenide-based porous materials is continuously expanding prompting investigations of the diverse functionality of these materials.[11-21]

So far, ternary or quaternary metal chalcogels have been synthesized mostly focusing on lighter chalcogenides, i.e. sulfides and selenides.[11-21] As far as tellurides are concerned, some binary telluride aerogels like PbTe,[22] CdTe,[23] or Bi_2Te_3 and only one example of a ternary aerogel $Bi_xSb_{2-x}Te_3$ have been reported.[24] In the present study, the sol–gel metathesis route is extended to quaternary tellurides. The new aerogel $KFeSbTe_3$ is composed of the trigonal pyramidal anion $SbTe_3^{3-}$ that connects Fe^{2+} ions to an anionic porous network with additional K^+ ions neutralizing the anionic $[FeSbTe_3]^-$-network. The resulting aerogel possess a high surface area and large

pore volume. A high adsorption capacity for toluene and CO_2 promise possible use of such materials in adsorptive separations.

Experimental

Materials

As starting materials tellurium (Alfa Aesar, 99.999 %), antimony (Strem Chemicals, 99.998 %), potassium (Strem Chemicals, 99 %), iron(II) acetate (Strem Chemicals, 97 % anhydrous), dimethyl formamide (Sigma, 99.8 % anhydrous), absolute ethanol (Aldrich, 99.8 %), toluene (Fisher Scientific, 99.9 %), cyclohexane (Roth Chemicals, 99.5 %) and cyclopentane (Roth Chemicals, 99.5 %) was used. High purity gases (N_2, He, CO_2, CH_4 and H_2) were obtained from Abdullah Hashim Industrial Gases & Equipment Co. Ltd. The ternary phase K_3SbTe_3 was prepared by reacting the elements in stoichiometric ratio at 550 ºC (100/K/h heating rate, 12 h soaking at 550 ºC, cooling to RT in 1d) (supporting information, Fig S1a).[25a] The solvents were degassed by bubbling N_2 gas through them for about 2 h before taking them into a nitrogen-filled glovebox ($c(O_2)$ < 0.1 ppm, $c(H_2O)$ < 0.1 ppm). Synthesis and solvent exchange of $KFeSbTe_3$ was carried out in the glovebox.

Synthesis of $KFeSbTe_3$ aerogel

For the synthesis of the $KFeSbTe_3$ chalcogel, 44 mg (0.25 mmol) of $Fe(CH_3CO_2)_2$ was dissolved under inert atmosphere in 4.0 mL of DMF. The light yellow solution of iron acetate was slowly added with stirring to a brown solution of 155 mg (0.25 mmol) of K_3SbTe_3 in 4.0 mL of DMF under inert atmosphere. The reaction mixture turned immediately into a black clear solution which was left at room temperature undisturbed for one week for gel formation. After one week, a black $KFeSbTe_3$ rigid chalcogel was obtained and solvent exchange was carried out with absolute ethanol 8-10 times over a week followed by supercritical CO_2 drying. After critical point drying, the obtained aerogel consists of a very fluffy black solid.

Supercritical drying

Supercritical drying was performed in a Tousimis Autosamdri–815B instrument. The sample was prepared in the glovebox using a small particle holder equipped with a 2 µm fine particle screen and transferred to the critical point dryer in a sealed container. The sample was soaked with liquid CO_2 and flushed 15-18 times over a period of 8 h (for 10 cm^3 sample) below 10 °C to completely remove the ethanol from the wet gel. The aerogel was obtained after supercritical drying at 35 ºC.

Characterization of the aerogel

Scanning electron microscopy/Energy dispersive X-ray spectroscopy (SEM/EDS)

SEM and EDS of the aerogel were performed on a Quanta 3D FEG. Powdered aerogel samples were analyzed on a carbon tape.

Transmission electron microscopy (TEM)

TEM samples were prepared by suspending the powder aerogel samples in absolute ethanol and then casting on carbon-coated Cu grid. High-resolution TEM images were obtained using a FEI Titan 80-300 Super Twin operated at 300 kV.

Adsorption measurements

All physisorption measurements were carried out on a Micromeritics ASAP 2020 HD instrument with Kalrez modification.

Nitrogen. Nitrogen adsorption and desorption isotherms were performed at 77 K. About 100-200 mg of sample was taken for each analysis. Before the analysis, samples were degassed at 348 K under vacuum ($<10^{-4}$ mbar) for 10 h. Low pressure incremental dosing of 0.1338 mmol/g (STP) and 30s equilibration were applied as analysis conditions. The BET transform plot was obtained in the 0.05 to 0.35[25b] relative pressure (P/Po) region and a correlation coefficient of 0.99999 was obtained in all of the cases while the distribution of pore sizes was calculated using the Barrett-Joyner-Halenda (BJH) model.

Hydrogen, Methane, and Carbon Dioxide. A cryogenic water bath (50:50 vol % water-ethylene glycol mixture) controlled by a Julabo HE digital chiller system was used for each measurement at 273 K and 263 K. Low-pressure incremental dosing of 0.022 mmol/g (STP) and 60 s of equilibration were used for each analysis.

Toluene, Cyclohexane, and Cyclopentane. The vapor adsorption studies of volatile hydrocarbons were carried out at 293(2) K. Low-pressure incremental dosing of 0.089 mmol/g (STP) and maximum 120 s of equilibration were used for each analysis.

Thermogravimetric analysis (TGA)

TGA measurements were performed using a Netzsch STA 449 F3 thermogravimetric analyzer with a heating rate of 20 K/min under N_2 flow (20 mL/min). The sample preparation was carried out in the glovebox using Al sample pans with a punctured lid.

Density measurement

The skeletal density of the aerogel was determined by a Micromeritics AccuPyc 1340 gas pycnometer using ultra high purity helium gas.

Powder diffraction

The powder diffraction patterns were recorded on a Stoe STADI MP powder diffractometer at 293(2) K, equipped with a Mythen 1K silicon strip detector covering 80° in 2θ and using Cu-$K\alpha_1$ radiation. The calibration was done with a silicon standard. The diffraction patterns (raw data) were compared to the simulated phases deposited in the Fachinformationszentrum Karlsruhe, Germany (Findit, release 2014).

UV/VIS spectroscopy

The UV/Vis diffuse reflectance spectrum was recorded with a Agilent Cary 5000 spectrometer in the wavelength range of 200-3000 nm. $BaSO_4$ powder was used as a reference (100% reflectance) material and for dilution of the sample.

Results and discussion

The $KFeSbTe_3$ chalcogel was obtained via the sol–gel method by the reaction of K_3SbTe_3 with anhydrous $Fe(OAc)_2$ in dried DMF. After keeping the reaction mixture undisturbed for 1 week, a black gel was obtained according to the following metathesis reaction (Scheme 1) and the solvent exchange was carried out with absolute ethanol 8-10 times followed by supercritical CO_2 drying. This process helps to remove the majority of the solvent from the pores retaining the gel porous network.[11-21] After drying, the obtained aerogel consists of a very fluffy solid. As previously reported, gel formation depends

significantly on the various reaction conditions, i.e., the choice of a suitable solvent, precursors, and reaction temperature.[14-16] Moreover, the proper selection of a suitable solvent to completely dissolve the precursors is an important criterion towards gelation. The metathesis reaction of K_3SbTe_3 with $Fe(OAc)_2$ was carried out in anhydrous DMF due to the moisture sensitivity of the ternary phase K_3SbTe_3.

$$Fe(OAc)_2 + K_3SbTe_3 \xrightarrow[7\ days]{DMF} KFeSbTe_3 + 2K(OAc)$$

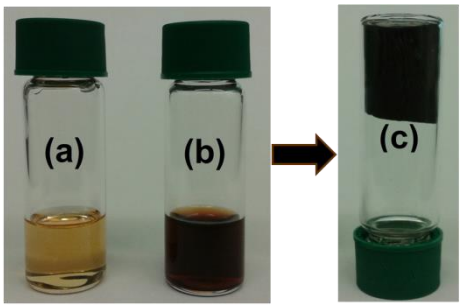

Scheme 1 Synthesis of the $KFeSbTe_3$ aerogel along with photographic illustration (DMF = dimethylformamide), (a) iron acetate solution in DMF, (b) K_3SbTe_3 (inorganic building block) solution in DMF, (c) completed metathesis reaction yielding a black chalcogel $KFeSbTe_3$.

The transmission electron microscopy (TEM) and the scanning electron microscopy images of the chalcogel showed the spongy nature of the gel (Fig 1 inset and supporting information, Fig S2). It has been observed that the introduction of the trigonal pyramidal telluride precursor into the chalcogenide network resulted in the formation of the new chalcogel $KFeSbTe_3$ with a BET surface area of 652 m^2/g. To the best of our knowledge this represents the largest BET surface area reported so far for chalcogenide-based aerogels.[11-24] The $KFeSbTe_3$ chalcogel was synthesized several times. The measurement was repeated three times on three different batches resulting in BET surface area measurements of 652, 647, 649 m^2/g. The interlinked porous nature of the metal chalcogel has been shown by the TEM images (Fig 1). In order to confirm the chemical composition of the chalcogel, multiple EDS analyses were performed to determine the relative atomic ratios of each element. In the dried $KFeSbTe_3$ gel, the elements K, Fe, Sb, and Te are present with an average ratio K/Fe/Sb/Te of 1:1.03:1.05:3.06 (Fig 1a and supporting information, Fig S2). Therefore, the average composition of the aerogel can be written as "$KFeSbTe_3$". The $KFeSbTe_3$ aerogel is related to $RbHgSbTe_3$ which crystallizes in the $KCuZrS_3$ structure type.[26a] The crystal structure of $RbHgSbTe_3$ consists of undulated layers of edge- and corner-sharing $SbTe_6$ octahedra. In the $KFeSbTe_3$ aerogel, it is assumed that an irregular distribution of iron atoms above and below the $SbTe_6$ layer could be the reason for pore formation. In order to get an idea about the structural chemistry of the $KFeSbTe_3$ aerogel, a solvothermal reaction was also attempted under similar conditions as described for the synthesis of $RbHgSbTe_3$.[26a] However; we could get only a mixture of some binary phases (supporting information, Fig S3) instead of a crystalline quaternary phase $KFeSbTe_3$. Therefore, we assume that the mild reaction conditions employed in gel formation make the aerogel a kinetic intermediate en route to the $KCuZrS_3$ structure type. The nitrogen adsorption and desorption isotherms of the prepared aerogel exhibits the type IV adsorption branch with a combination of H1 and H3 hysteresis loops characteristic of a mesoporous system (Fig 1b).[14-16,26b] The existence of a combination of H1 and H3 type hysteresis loops reveals adsorption and desorption do not follow the same pathway, and mesopores have significant fractions of cylindrical and slit-shaped geometries.[26b] The Barrett–Joynes–Halenda (BJH)[25b] plot of pore size distribution shows a broad range of pore sizes from 1.7–175 nm (Fig 2a) with an average pore diameter of 18.5 nm. The skeletal density of the material 2.02 g/cm^3 has been determined by pycnometry.

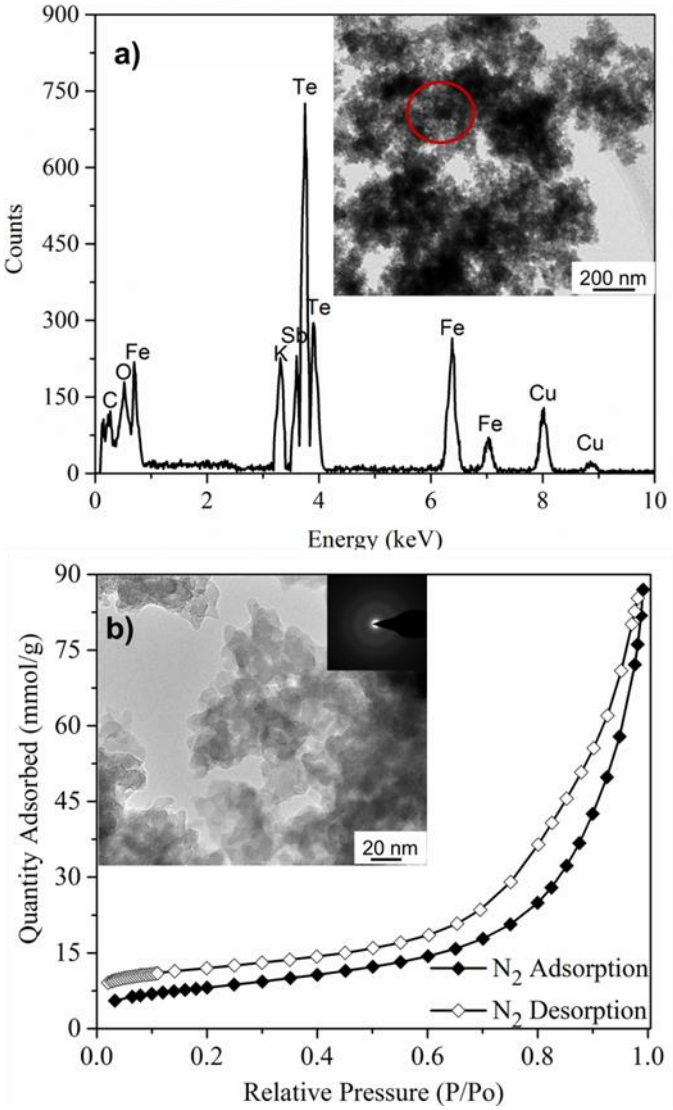

Fig. 1 TEM images and STEM-XEDS spectra of the $KFeSbTe_3$ aerogel. (a) Low magnification TEM image (inset) with STEM-XEDS spectra of the spot analysis, (b) High magnification TEM image showing porosity and amorphous nature by electron diffraction (inset) with N_2 adsorption-desorption isotherm.

The TEM micrographs of the aerogel sample clearly show the random porous agglomeration of the nanoparticles (Fig 1a-b inset). The TEM images show pores from micro (below 2 nm), meso (2-50 nm), to macro (above 50 nm) regions. Electron diffraction of these particles revealed diffuse scattering, which indicates their amorphous nature (Fig 1b inset). The absence of any structure directing agent or template has revealed that the pores are diverse in shape and size forming voids rather than regular channels within the aerogel framework. Such a random porous interconnected network is characteristic for the chalcogenide-based aerogel structures.[11,18] Nanoparticles are found with an average diameter of 9.2 nm. The powder X-ray diffraction pattern of the $KFeSbTe_3$ chalcogel shows a predominantly amorphous nature and no significant crystalline phase

has been observed (supporting information, Fig S1b). As shown in Fig 1b inset, electron diffraction of the sample also showed only diffuse scattering indicating a random aperiodic structure and these observations are in good agreement with the powder X-ray diffraction results.

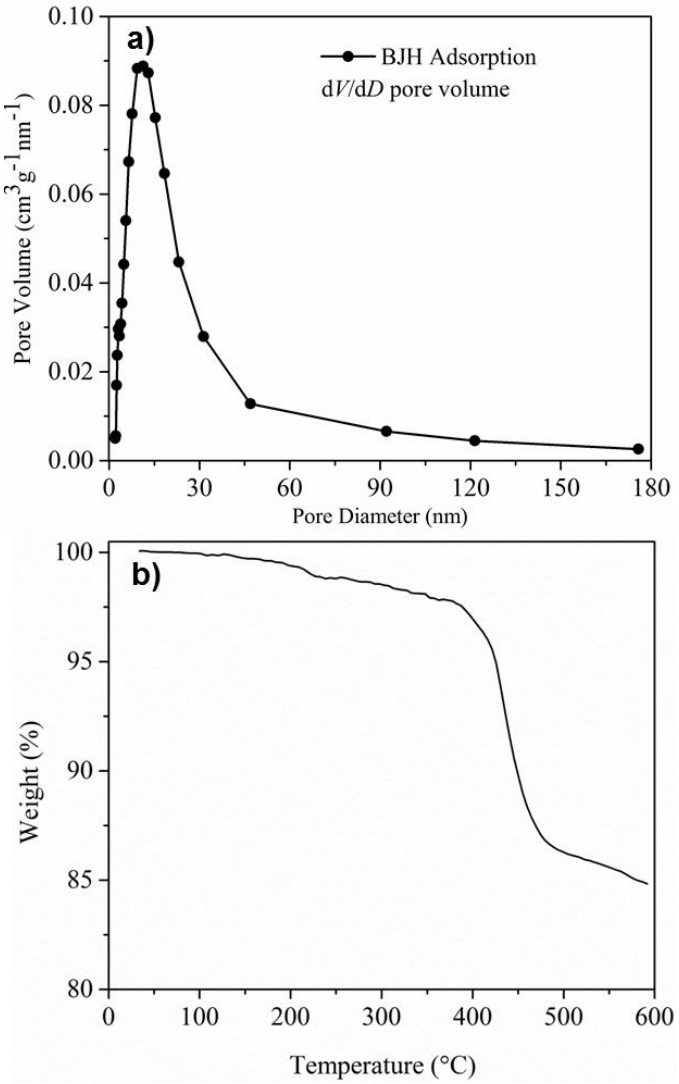

Fig. 2 (a) Pore-size (V-D) distribution plot calculated from the adsorption isotherm by the BJH method, (b) Thermogravimetric analysis of the $KFeSbTe_3$ aerogel showing a gradual weight loss.

The $KFeSbTe_3$ chalcogel is air sensitive but shows a good thermal stability up to 400 °C. TGA shows a minor weight loss about 1-2 % in the temperature range from 100-400 °C, which is caused by the evaporation of the adsorbed residual solvent (Fig 2b). Afterwards, its decomposition to tellurium has been observed up to 600 °C. Normally, from ~200-600 °C, the loss of chalcogen or decomposition to chalcogen is common in chalcogels.[15,16,18b] After TGA, the remaining substance has been characterized by powder X-ray diffraction which shows that FeTe is present as a major crystalline phase (supporting information, Fig S4).

From the electronic absorption spectra, the optical energy bandgap of the aerogel was determined by diffuse reflectance solid-state spectroscopy showing a value of ca. 2.12 eV (supporting information, Fig S5).

Adsorption studies

The $KFeSbTe_3$ aerogel has been analyzed by the adsorption isotherms using volatile hydrocarbons like toluene, cyclohexane and cyclopentane as probe molecules (Fig 3).

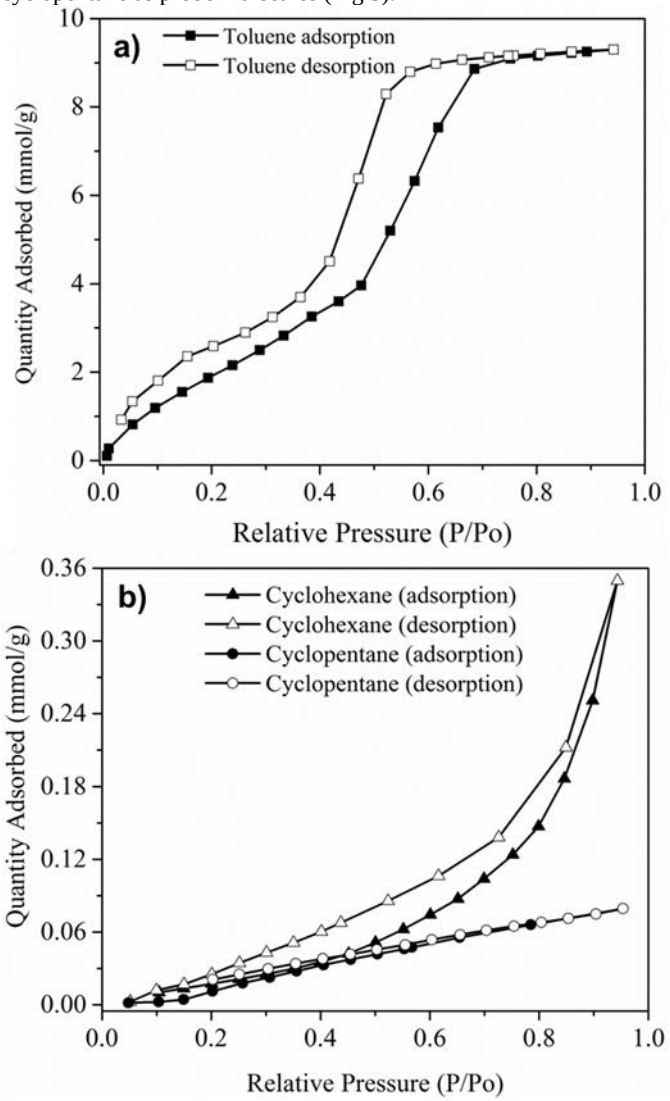

Fig. 3 Adsorption isotherms of the volatile hydrocarbons observed in $KFeSbTe_3$ chalcogel at 293 (2) K. (a) toluene, (b) cyclohexane and cyclopentane.

It has been observed that the aerogel shows much higher adsorption affinity for toluene compared to other hydrocarbons. This preferential uptake might be explained on the basis of the cation–π interaction where iron can interact with toluene molecules which can enhance the adsorption affinity. Such interactions have been reported in MIL-101 which shows higher adsorption affinity to toluene than *n*-hexane.[27] In agreement with the relative polarity (polarity index)[11] higher adsorption of toluene (polarity index: 2.4), less for cyclohexane (polarity index: 0.2) and the least for cyclopentane (polarity index: 0.1) was observed. This behavior can be explained on the basis of the surface polarizability of the chalcogel and relative polarity of the volatile solvents. Moreover, it has been noticed that the aerogel exhibits minor adsorption at low relative pressures ($0 < P/Po < 0.5$), indicating that only a small portion of the adsorption occurs in microporous region ($d \leq 2$ nm). It indicates that significant adsorption takes place at higher relative pressures ($P/Po > 0.5$) where meso- ($2 < d < 50$ nm) and macropores ($d > 50$ nm) are playing the major role. Comparing the adsorption capacity of the toluene vapors

in $KFeSbTe_3$ aerogel with different porous materials, it is noteworthy that the toluene adsorption capacity in $KFeSbTe_3$ is 3–6 times larger than that of zeolites, activated carbon, and silica gel (supporting information, Table S1).[6] The adsorption capacity for toluene was also found to be 1.5–3.5 times higher than the capacity of some metal organic frameworks (MOFs) like $Cu_3(BTC)_2$,[28] MOF-177 and MIL-100,[29] as well as some polyoxometalate MOFs[28] and similar to the toluene adsorption capacity of MIL-101[30] (supporting information, Table S1). The efficiency of toluene desorption can reach up to 91 % exhibiting a reasonable reversibility of toluene adsorption–desorption.

The experimental evidence presented here on the preferential adsorption of organic molecules in $KFeSbTe_3$ suggests a potential application of such materials in the separation of aromatics from aliphatic hydrocarbons at relatively low temperatures, i.e., room temperature. Because of the higher adsorption capacity of toluene, such porous materials could also be useful for catalytic oxidation of toluene to several oxygenates like benzyl alcohol, benzaldehyde, benzoic acid, and benzoate etc.[31] Moreover, the synthesized chalcogel might be valuable for the design of an adsorption-based process for the disposal of wastes containing volatile organic compounds (VOCs) which are the most common air pollutants.[32]
Tests of the $KFeSbTe_3$ aerogel adsorption capability for different gases like CO_2, CH_4 and H_2 at 273 K and 263 K show the highest adsorption for CO_2 (Fig 4a and supporting information Fig S6). This fact can also be explained on the basis of the polarizability. CO_2 is more polarizable than CH_4 and H_2 (polarizability α in units of 10^{-24} cm^3: α (CO_2) = 2.9 > α (CH_4) = 2.6 > α (H_2) = 0.8), and interactions with the chalcogenide surface through dispersion forces are stronger than those of the other investigated gas adsorptives.[19] From the adsorption isotherms of CO_2, CH_4 and H_2, the adsorption selectivity of an equimolar gas mixture in the chalcogel has been calculated according to the ideal adsorbed solution theory (IAST; Fig 4b, supporting information, Fig S7-8, Table S2-3).[16,19] The calculations revealed that the selectivities of the gas pairs CO_2/H_2 and CO_2/CH_4 are 121 and 75 respectively (Fig 4 and supporting information, Fig S7-8). This illustrates the large difference in the adsorbed amount of CO_2 in comparison to H_2 or CH_4. The selectivity for CO_2 over H_2 is much higher than selectivity previously predicted by the IAST for zeolites[33], some MOFs (e.g., MOF-5 and Cu-BTC)[34] and most of the chalcogels (Table S2).[15,16,19] These findings also indicate the potential suitability of the $KFeSbTe_3$ chalcogel for gas separation (especially separation of CO_2 from H_2 during the water gas shift reaction).

Conclusions

In summary, the metathesis reaction between $Fe(OAc)_2$ and the ternary phase K_3SbTe_3 gave rise to the high surface area chalcogel $KFeSbTe_3$, which shows preferential adsorption of polarizable hydrocarbons and gases. The adsorption capacities of the three volatile hydrocarbons are found in the following order: toluene > cyclohexane > cyclopentane. The preferential adsorption of organic molecules in the chalcogel suggests a possible application for the separation of aromatics from aliphatic hydrocarbons at relatively low temperatures, i.e., room temperature. Because of the higher adsorption capacity of toluene, such porous materials could also be useful for catalytic oxidation reactions or for removal of VOCs which are the most common air pollutants. Toluene is known as one of the most representative VOCs because of its high POCP (photochemical ozone creativity potential) and adverse effect on human health.[32] The preferential uptake of volatile hydrocarbons and gaseous species in chalcogel promises this kind of material for a broad set of applications such as separation processes, environmental decontamination and catalysis. The extension of the sol-gel synthetic scheme suggests that new functional materials with high surface area could also be accessible using soluble precursors and transition metal ions.

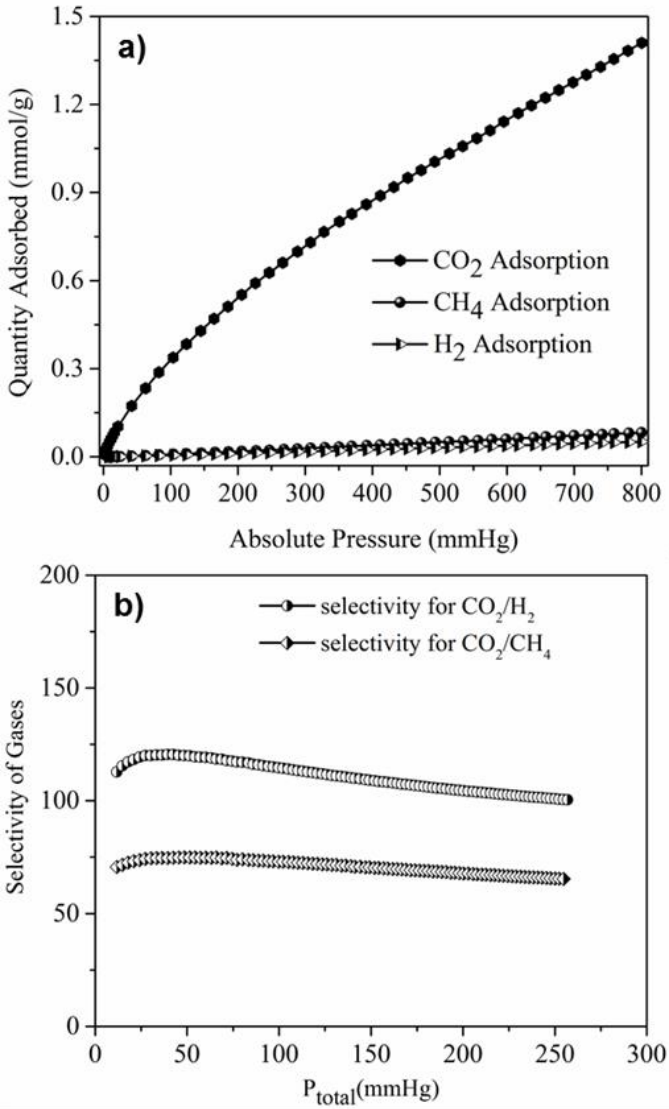

Fig. 4 (a) Adsorption isotherms of CO_2, CH_4 and H_2 observed in $KFeSbTe_3$ at 273 K, (b) Selectivity of CO_2 over H_2 and CO_2 over CH_4 in $KFeSbTe_3$ as predicted by IAST for equimolar mixtures of CO_2/H_2 and CO_2/CH_4 at 273 K (P_{total} is the total pressure of the gas mixture).

Acknowledgements

We wish to thank Mr. V. Q. Wang for TEM images and Dr M. N. Hedhili for XPS Measurements. This research was supported by the King Abdullah University of Science and Technology (KAUST) baseline funding.

Notes and references

Physical Sciences and Engineering Division, King Abdullah University of Science and Technology Thuwal, Kingdom of Saudi Arabia.
Email: alexander.rothenberger@kaust.edu.sa.

† Electronic Supplementary Information (ESI) available: SEM/EDS results, powder diffraction patterns, adsorption capacity tables, gases selectivity data, IAST calculations, XPS experimental details and results

are available in the form of supplementary information associated with this article. See DOI: 10.1039/b000000x/

References

1. R. T. Yang, *Adsorbents: Fundamentals and Applications*, Wiley, New York, 2007.
2 . D. M. Ruthven, *Principles of adsorption and adsorption processes*, John Wiley, New York, 1984.
3. B. Van de Voorde, B. Bueken, J. Denayer and D. De Vos, *Chem. Soc. Rev.*, 2014, **43**, 5766-5788.
4. C. R. Vitasari, G. W. Meindersma and A. B. de Haan, *Green Chem.*, 2012, **14**, 321-325.
5. J. R. Li, J. Sculley and H. C. Zhou, *Chem. Rev.*, 2012, **112**, 869-932.
6. C. M. Wang, K. S. Chang, T. W. Chung and H. D. Wu, *J. Chem. Eng. Data*, 2004, **49**, 527-531.
7. E. C. de Oliveira, C. Pires and H. O. Pastore, *J. Braz. Chem. Soc.*, 2006, **17**, 16-29.
8. E. J. Simpson, R. K. Abukhadra, W. J. Koros and R. S. Schechter, *Ind. Eng. Chem. Res.*, 1993, **32**, 2269-2276.
9. V. A. Likholobov, V. B. Fenelonov, L. G. Okkel, O. V. Goncharova, L. B. Avdeeva, V. I. Zaikovskii, G. G. Kuvshinov, V. A. Semikolenov, V. K. Duplyakin, O. N. Baklanova and G. V. Plaksin, *React. Kinet. Catal. Lett.*, 1995, **54**, 381-411.
10. Z. R. Herm, E. D. Bloch and J. R. Long, *Chem. Mater.*, 2014, **26**, 323-338.
11. (a) E. Ahmed and A. Rothenberger, *Microporous Mesoporous Mater.*, 2014, **199**, 74-82; (b) E. Ahmed, J. Khanderi, D. H. Anjum and A. Rothenberger, *Chem. Mater.*, 2014, **26**, 6454-6460.
12. S. L. Brock, I. U. Arachchige and K. K. Kalebaila, *Comments Inorg. Chem.*, 2006, **27**, 103-126.
13. I. U. Arachchige and S. L. Brock, *Acc. Chem. Res.*, 2007, **40**, 801-809.
14. S. Bag, P. N. Trikalitis, P. J. Chupas, G. S. Armatas and M. G. Kanatzidis, *Science*, 2007, **317**, 490-493.
15. S. Bag, A. F. Gaudette, M. E. Bussell and M. G. Kanatzidis, *Nat. Chem.*, 2009, **1**, 217-224.
16. S. Bag and M. G. Kanatzidis, *J. Am. Chem. Soc.*, 2010, **132**, 14951-14959.
17. I. R. Pala, I. U. Arachchige, D. G. Georgiev and S. L. Brock, *Angew. Chem. Int. Ed.*, 2010, **49**, 3661-3665.
18. (a) M. Shafaei-Fallah, J. Q. He, A. Rothenberger and M. G. Kanatzidis, *J. Am. Chem. Soc.*, 2011, **133**, 1200-1202; (b) Y. Oh, C. D. Morris and M. G. Kanatzidis, *J. Am. Chem. Soc.*, 2012, **134**, 14604-14608.
19. M. Shafaei-Fallah, A. Rothenberger, A. P. Katsoulidis, J. He, C. D. Malliakas and M. G. Kanatzidis, *Adv. Mater.*, 2011, **23**, 4857-4860.
20. K. Polychronopoulou, C. D. Malliakas, J. Q. He and M. G. Kanatzidis, *Chem. Mater.*, 2012, **24**, 3380-3392.
21. B. J. Riley, J. Chun, W. Um, W. C. Lepry, J. Matyas, M. J. Olszta, X. Li, K. Polychronopoulou and M. G. Kanatzidis, *Environ. Sci. Technol.*, 2013, **47**, 7540-7547.
22. S. Ganguly and S. L. Brock, *J. Mat. Chem.*, 2011, **21**, 8800-8806.
23. (a) T. Hendel, V. Lesnyak, L. Kuhn, A. K. Herrmann, N. C. Bigall, L. Borchardt, S. Kaskel, N. Gaponik and A. Eychmueller, *Adv. Funct. Mater.*, 2013, **23**, 1903-1911; (b) D. S. Dolzhnikov, H. Zhang, J. Jang, J. S. Son, M. G. Panthani, T. Shibata, S. Chattopadhyay, D. V. Talapin, *Science*, 2015, **347**, 425-428.
24. S. Ganguly, C. Zhou, D. Morelli, J. Sakamoto and S. L. Brock, *J. Phys. Chem. C*, 2012, **116**, 17431-17439.
25. (a) J. S. Jung, B. O. Wu, E. D. Stevens and C. J. Oconnor, *J. Solid State Chem.*, 1991, **94**, 362-367; (b) I. F. Rouquerol, J. Rouquerol and K. Sing, *Adsorption by Powders and Porous Solids: Principles, Methodology, and Applications*, Academic Press, San Diego, CA, 1999.
26. (a) J. Li, Z. Chen, X. Wang and D. M. Proserpio, *J. Alloys Comp.* 1997, **262-263**, 28-33; (b) K. S. W. Sing, D. H. Everett, R. A. W. Haul, L. Moscou, R. A. Pierotti, J. Rouquerol and T. Siemieniewska, *Pure Appl. Chem.*, 1985, **57**, 603-619.
27. C.-Y. Huang, M. Song, Z.-Y. Gu, H.-F. Wang and X.-P. Yan, *Environ. Sci. Technol.*, 2011, **45**, 4490-4496.
28. F. J. Ma, S. X. Liu, D. D. Liang, G. J. Ren, F. Wei, Y. G. Chen and Z. M. Su, *J. Solid State Chem.*, 2011, **184**, 3034-3039.
29. Y.-K. Seo, J. W. Yoon, J. S. Lee, U. H. Lee, Y. K. Hwang, C.-H. Jun, P. Horcajada, C. Serre and J.-S. Chang, *Microporous Mesoporous Mater.*, 2012, **157**, 137-145.
30. K. Yang, Q. Sun, F. Xue and D. H. Lin, *J. Hazard. Mater.*, 2011, **195**, 124-131.
31. S. S. Acharyya, S. Ghosh, R. Tiwari, B. Sarkar, R. K. Singha, C. Pendem, T. Sasaki and R. Bal, *Green Chem.*, 2014, **16**, 2500-2508.
32. M. Ousmane, L. F. Liotta, G. Di Carlo, G. Pantaleo, A. M. Venezia, G. Deganello, L. Retailleau, A. Boreave and A. Giroir-Fendler, *Appl. Catal. B-Environ.*, 2011, **101**, 629-637.
33. C. D. Boisgontier, J. Parmentier, A. Faour, J. Patarin and G. D. Pringruber, *Energy Fuels*, 2010, **24**, 3595-3602.
34. (a) Q. Yang and C. Zhong, *J. Phys. Chem. B*, 2006, **110**, 17776-17783; (b) Z. Zhao, Z. Li and Y. S. Lin, *Ind. Eng. Chem. Res.*, 2009, **48**, 10015-10020.

Graphical Abstract

A first quaternary telluride aerogel $KFeSbTe_3$ is described which comprises high surface area for selective uptake of toluene and CO_2.